Prediction rules for the detection of coronary artery plaques: evidence from cardiac CT

Saur, S C ; Cattin, P C ; Desbiolles, L ; Fuchs, T J ; Székely, G ; Alkadhi, H

Abstract: OBJECTIVES: To evaluate spatial plaque distribution patterns in coronary arteries based on computed tomography coronary angiography data sets and to express the learned patterns in prediction rules. An application is proposed to use these prediction rules for the detection of initially missed plaques. MATERIAL AND METHODS: Two hundred fifty two consecutive patients with chronic coronary artery disease underwent contrast-enhanced dual-source computed tomography coronary angiography for clinical indications. Coronary artery plaques were manually labeled on a 16-segment coronary model and their position (ie, segments and bifurcations) and composition (ie, calcified, mixed, or noncalcified) were noted. The frequent itemset mining algorithm was used to statistically search for plaque distribution patterns. The patterns were expressed as prediction rules: given plaques at certain locations as conditions, a prediction rule gave evidence–with a certain confidence value–for a plaque at another location within the coronary artery tree. Prediction rules with the highest confidence values were evaluated and described. Furthermore, to improve manual plaque detection, all prediction rules were applied on the patient data to search for segments with potentially missed plaques. These segments were then reviewed in a second, guided reading for the existence of plaques. The same number of segments was also determined by a weighted random approach to evaluate the quality of prediction resulting from frequent itemset mining. RESULTS: In 200 of 252 (79.4%) patients, at least one coronary plaque (range, 1-22 plaques) was found. In total 1229 plaques (990 calcified, 80.6%; 227 mixed, 18.5%; 12 noncalcified, 1%) distributed, over 916 coronary segments and 507 vessels were manually labeled. Four plaque distribution patterns were identified: 20.6% of the patients had no plaques at all; 31.7% had plaques in the left coronary artery tree; 46.4% had plaques both in left and right coronary arteries, whereas 1.2% of the patients had plaques solely in the right coronary artery (RCA). General rules were found predicting plaques in the left anterior descending artery (LAD), given plaques in segments of the RCA or in the left main artery. Further general rules predicted plaques in the LAD, given plaques in the circumflex artery. In the guided review, the segment selection based on the prediction rules from frequent itemset mining performed significantly better ($P < 0.001$) than the weighted random approach by revealing 48 initially missed plaques. CONCLUSIONS: This study demonstrates spatial plaque distribution patterns in coronary arteries as determined with cardiac CT. Use of the frequent itemset mining algorithm yielded rules that predicted plaques at certain sites given plaques at other sites of the coronary artery tree. Use of these prediction rules improved the manual labeling of coronary plaques as initially missed plaques could be predicted with the guided review.

DOI: https://doi.org/10.1097/RLI.0b013e3181a8afc4

Originally published at:
Saur, S C; Cattin, P C; Desbiolles, L; Fuchs, T J; Székely, G; Alkadhi, H (2009). Prediction rules for the detection of coronary artery plaques: evidence from cardiac CT. Investigative Radiology, 44(8):483-490.
DOI: https://doi.org/10.1097/RLI.0b013e3181a8afc4

Prediction Rules for the Detection of Coronary Artery Plaques

Evidence From Cardiac CT

Stefan C. Saur, MSc, Philippe C. Cattin, PhD,*† Lotus Desbiolles, MD,‡ Thomas J. Fuchs, MSc,§ Gábor Székely, PhD,* and Hatem Alkadhi, MD‡*

Objectives: To evaluate spatial plaque distribution patterns in coronary arteries based on computed tomography coronary angiography data sets and to express the learned patterns in prediction rules. An application is proposed to use these prediction rules for the detection of initially missed plaques.

Material and Methods: Two hundred fifty two consecutive patients with chronic coronary artery disease underwent contrast-enhanced dual-source computed tomography coronary angiography for clinical indications. Coronary artery plaques were manually labeled on a 16-segment coronary model and their position (ie, segments and bifurcations) and composition (ie, calcified, mixed, or noncalcified) were noted. The frequent itemset mining algorithm was used to statistically search for plaque distribution patterns. The patterns were expressed as prediction rules: given plaques at certain locations as conditions, a prediction rule gave evidence—with a certain confidence value—for a plaque at another location within the coronary artery tree. Prediction rules with the highest confidence values were evaluated and described. Furthermore, to improve manual plaque detection, all prediction rules were applied on the patient data to search for segments with potentially missed plaques. These segments were then reviewed in a second, guided reading for the existence of plaques. The same number of segments was also determined by a weighted random approach to evaluate the quality of prediction resulting from frequent itemset mining.

Results: In 200 of 252 (79.4%) patients, at least one coronary plaque (range, 1–22 plaques) was found. In total 1229 plaques (990 calcified, 80.6%; 227 mixed, 18.5%; 12 noncalcified, 1%) distributed, over 916 coronary segments and 507 vessels were manually labeled. Four plaque distribution patterns were identified: 20.6% of the patients had no plaques at all; 31.7% had plaques in the left coronary artery tree; 46.4% had plaques both in left and right coronary arteries, whereas 1.2% of the patients had plaques solely in the right coronary artery (RCA). General rules were found predicting plaques in the left anterior descending artery (LAD), given plaques in segments of the RCA or in the left main artery. Further general rules predicted plaques in the LAD, given plaques in the circumflex artery. In the guided review, the segment selection based on the prediction rules from frequent itemset mining performed significantly better ($P < 0.001$) than the weighted random approach by revealing 48 initially missed plaques.

Conclusions: This study demonstrates spatial plaque distribution patterns in coronary arteries as determined with cardiac CT. Use of the frequent itemset mining algorithm yielded rules that predicted plaques at certain sites given plaques at other sites of the coronary artery tree. Use of these prediction rules improved the manual labeling of coronary plaques as initially missed plaques could be predicted with the guided review.

Key Words: coronary artery, plaque, computed tomography, spatial distribution, prediction rules

(*Invest Radiol* 2009;44: 483–490)

Atherosclerotic cardiovascular diseases represent one of the leading causes of morbidity and mortality in developed countries. In the presence of atherosclerotic coronary artery disease (CAD), plaques develop by the accumulation of lipid or calcified deposits in the coronary vessel walls. The imaging finding of coronary lumen narrowing typically correlates with the presence of stable symptomatic disease caused by restricted blood supply to the myocardium.[1] Another manifestation of CAD is acute coronary syndrome with myocardial infarction or sudden cardiac death that often is caused by the disruption of coronary plaques and subsequent thrombus formation.[2,3] Beyond the degree of luminal narrowing, plaque composition (ie, calcified, noncalcified, or mixed plaques)[4–6] and plaque localization[7–10] represent additional major determinants of the risk of developing the various clinical manifestations of CAD. Thus, characterization of coronary obstruction, plaque morphology, and plaque location is important for detecting and stratifying the risk of patients with CAD.[11]

The imaging reference standard for the detection and characterization of coronary artery plaques is intravascular ultrasound (IVUS). Owing to its excellent spatial and contrast resolution, IVUS is able to characterize and classify coronary artery plaques with a high accuracy as compared with histopathology.[12,13] However, IVUS is a considerably invasive procedure and, in addition, is not able to depict the vessel wall in more distal coronary segments because of the relatively large diameter of the device.

Recently, computed tomography coronary angiography (CTCA) has emerged as a robust and accurate modality for the noninvasive assessment of coronary arteries with respect to the presence or absence of coronary artery stenoses.[14–16] Being a cross-sectional imaging modality, CTCA also allows for the detection and characterization of coronary plaques.[17–20] Various recent studies have demonstrated different plaque type compositions as determined with CT to be associated with different manifestations of CAD, ie, acute coronary syndrome or stable angina.[17] Furthermore, the importance of plaque detection and quantification by CTCA has been recently highlighted through demonstration of its prognostic value in patients with known or suspected CAD.[21] However, CTCA depicts only the majority but not all coronary plaques in comparison with IVUS. This was explained by the still limited spatial, temporal, and contrast resolution of current CT technology.[11] Another explanation for the lower performance of CTCA in comparison with IVUS has been suggested to be the considerable intra- and interobserver variability for the detection and differentiation of plaques with CTCA.[22]

Received January 5, 2009, and accepted for publication, after revision, March 29, 2009.

From the *Computer Vision Laboratory, ETH Zurich, Zurich, Switzerland; †Medical Image Analysis Center, University of Basel, Basel, Switzerland; ‡Institute of Diagnostic Radiology, University Hospital Zurich, Zurich, Switzerland; and §Department of Computer Science, ETH Zurich, Zurich, Switzerland.

Supported by the National Center of Competence in Research, Computer Aided and Image Guided Medical Interventions of the Swiss National Science Foundation available at: (http://co-me.ch).

Reprints: Hatem Alkadhi, MD, Institute of Diagnostic Radiology, University Hospital Zurich, Raemistrasse 100, 8091 Zurich, Switzerland. E-mail: hatem.alkadhi@usz.ch.

ISSN: 0020-9996/09/4408-0483

The purpose of this study was to search for spatial distribution patterns of coronary artery plaques using CTCA data sets. Based on these patterns, prediction rules of plaque distributions were extracted. These rules were then used for a targeted review of coronary segments in a second reading with regard to potentially missed plaques.

MATERIALS AND METHODS

Patients

Between August 2007 and December 2007, 252 consecutive patients (166 male, 86 female, age 64.5 ± 11.6 years, range: 28–88 years) who underwent CTCA for clinical indications were enrolled for this study. Demographic data and clinical characteristics of the patients are summarized in Table 1. All patients had a low- to intermediate pretest probability of having CAD and suffered from typical angina (15.9%), atypical angina (26.6%), or nonanginal chest pain (57.5%). None of the patients suffered from unstable angina. All patients were referred for ruling-out significant coronary stenoses. Patients with known allergy to iodinated contrast agent, serum creatinine greater than 1.5 mg/dL, glucophage (metformin) treatment, and hyperthyroidism were excluded from study enrolment. This retrospective study was approved by the local ethics committee who waived the written informed consent requirement.

TABLE 1. Patient Demographics and Clinical Characteristics of the Study Population

	Total
No. patients	252 (100%)
Age (yr)	64.5 ± 11.6 (28–88)
Male/female	166/86 (65.9%/34.1%)
BMI (kg/m^2)	25.7 ± 4.0 (19.1–34.1)
Heart rate (bpm)	67.3 ± 6.8 (51–88)
Risk factors	
Smoker	121 (48.0%)
Diabetes	29 (11.5%)
High serum cholesterol	110 (43.7%)
Arterial hypertension	160 (63.5%)
Positive family history	101 (40.1%)
Reasons for referral	
Typical angina	40 (15.9%)
Atypical angina	67 (26.6%)
Non anginal chest pain	145 (57.5%)

BMI indicates body mass index.

CT Protocol

All patients were scanned on a dual-source CT scanner (Somatom Definition, Siemens Medical Solutions, Forchheim, Germany) following a standard CTCA protocol. All patients received a single dose of 2.5 mg isosorbiddinitrate s. l. (Isoket, Schwarz Pharma, Monheim, Germany). No beta-receptor antagonists were given prior to CT. For CTCA, 80 mL of a nonionic, iodinated contrast agent (Ultravist 370, 370 mg/mL, Bayer Schering Pharma, Berlin, Germany) was injected at a flow rate of 5 mL/s followed by 30 mL saline solution through an antecubital vein. Contrast agent application was controlled by bolus tracking in the ascending aorta (signal attenuation threshold 100 HU). Scanning parameters were: detector collimation 32 × 0.6 mm, slice acquisition 64 × 0.6 mm by means of a z-flying focal spot, gantry rotation time 330 milliseconds, pitch of 0.2 to 0.5 depending on the heart rate (HR), tube current time product 330 mAs as per rotation, and tube potential 120 kV. The CT scans were performed from the level of the tracheal bifurcation to the diaphragm in a cranio-caudal direction. Electrocardiography-gated tube current modulation for radiation dose reduction was used in all patients.[23] CTCA scans were reconstructed using a mono-segment algorithm[24] with a slice thickness of 0.75 mm, a reconstruction increment of 0.4 mm, and using a soft-tissue convolution kernel (B26f) during mid-diastole at 70% of the RR interval. When motion artifacts were present in this data set, additional reconstructions were performed in 5% steps within the full tube current window.

Data Analysis

A graphical user interface has been developed with MeVisLab software (MeVis Research, Bremen, Germany) for the manual labeling of the coronary plaques. Patient information from all data sets was removed prior to the data analysis to allow for an anonymized read-out. A radiologist with 7 years of experience in cardiovascular radiology determined the type, position, and the degree of stenosis for each plaque. The position of the plaques were defined according to the scheme proposed by the American Heart Association.[25] In addition to the 16 segments, the 9 bifurcations of the model were also included as positions in this study, as bifurcations are preferred locations for the development of plaques.[26] A plaque was assigned to a bifurcation when it was centered in this location and did not extend more than 2 mm into adjacent coronary segments. If a plaque extended over more than one segment, it was labeled according to its most proximal position. In the following, the term segment will be equivalently used to refer to a segment or bifurcation. Segments were combined to vessels which in turn were summarized as branches of the coronary artery tree. Four vessels were differentiated: the right coronary artery (RCA) consisted of segment 1 through 4 with all the enclosed bifurcations. The left main artery (LM) was equivalent to segment 5 including its bifurcation

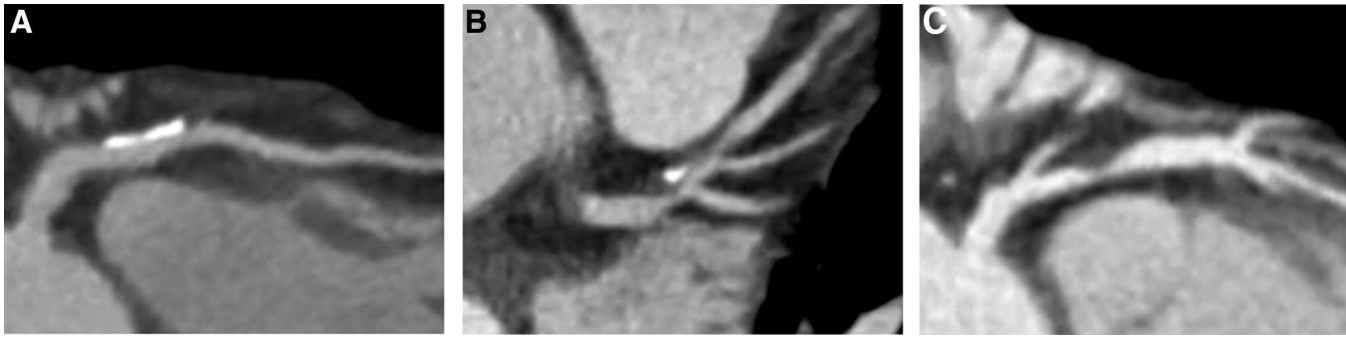

FIGURE 1. Examples of the 3 different types of plaques that were differentiated at CTCA: (A) purely calcified plaques, (B) mixed plaques indicating a mixture of calcified and noncalcified components, and (C) purely noncalcified plaques.

into the left anterior descending (LAD, segment 6–10), and circumflex (CX, segment 11–15) artery, respectively. Two branches were distinguished, namely the right coronary tree (RCA) and the left coronary tree composed of LM, CX, LAD, and segment 16.

Three different types of plaques were differentiated on a visual basis (using the soft tissue convolution reconstructions) at CTCA: purely calcified plaques, mixed plaques indicating a mixture of calcified and noncalcified plaques, and purely noncalcified plaques (Fig. 1). The plaques were further characterized as being obstructive, indicating a vessel diameter narrowing greater than 50%, or as nonobstructive, indicating a luminal narrowing below 50%, based on CTCA. The reader was allowed to adapt the window-level settings for the plaque analysis. Selected ranges for the width and the center were 1000 to 1600 and 350 to 500, respectively.

Spatial Plaque Distribution Patterns

The frequent itemset mining algorithm was used to test for spatial plaque distribution patterns.[27] The basic concept of this approach and the role of prediction rules that express correlations among the spatial distribution of plaques are briefly explained in the following section.

Frequent itemset mining was originally introduced for performing a market basket analysis.[27] The purpose of such an analysis is to derive patterns of products that are frequently bought together. For this, the items in customer's baskets are analyzed for a certain number of baskets. Afterward, so-called association rules can be derived that represent statistical correlations which are used to research the dependencies among items. An association rule expresses the probability that—given a set of items (itemset) in a basket–a certain other item is also present. Therefore, it can be used to predict the content of new baskets if only some items are given. Because of their predictive character, association rules are referred to as prediction rules in the following.

For the application of frequent itemset mining in this study, a patient "corresponded" to a basket. Multiple items such as the coronary segment, the coronary vessel, and the branch were assigned to each plaque to describe its position in different hierarchical levels.[28]

A prediction rule has the form "conditions → conclusion (support, confidence)" and refers to a relation between one or more items—the conditions—and one item as the conclusion. The expressiveness of a prediction rule is given by its support and confidence measure. The support of a prediction rule is the percentage of cases in which it applies in the observed population.[29] Thus, it is a measure of the generality of a prediction rule. The confidence of a prediction rule is the percentage of cases in which the rule is correct relative to the number of cases in which it is applicable, ie, the conditions are met.[27] For example a prediction rule "segment 6, segment 9 → segment 5 (35%, 93%)" means that plaques in segment 6 and segment 9 (found in 35% of all observations in the data set) indicate the existence of an additional plaque in segment 5 with a probability of 93%. If not stated otherwise, a minimum confidence value of 80% and a minimum support value of 15% were required for the prediction rules in this study.

Guided Review Based on Frequent Itemset Mining

Based on the results from frequent itemset mining giving rise to spatial plaque distribution patterns, the radiologist from the first reading was guided for a second read-out. The idea of this guided review was to avoid a complete second reading by reviewing only specific segments having a high probability of containing initially missed plaques, as predicted by the results from frequent itemset mining. The prediction rules were applied on each of the 252 data sets to search for additional plaques. Guided review by frequent itemset mining was used to extract a list of segments to be reviewed in the guided review. Therefore, it was tested if there were prediction rules indicating the presence of additional plaques in segments not labeled yet.

For comparison, the same number of segments was determined by a weighted random approach to evaluate the quality of the segment selection from frequent itemset mining. This weighted random approach selected segments by considering only the probability of occurrence for a plaque in a specific position. It was the most intuitive way to select segments for review: those segments where many plaques were observed in the first labeling have a higher probability of containing missed plaques in general and are therefore selected with higher frequency for review.

The reader from the initial labeling was then asked to review the selected segments from frequent itemset mining and the weighted random approach for the presence of missed plaques. For this second reading, the reader was blinded to the approach that selected the segment. To ascertain the presence of the initially missed plaques that were detected in the second reading, a second radiologist (also with 7 years of experience in cardiovascular imaging) was consulted for consensus. The guided review was performed 3 months after the initial labeling.

Statistical Analysis

All statistical analyses were performed using the software package R (release 2.8.0 for Windows, available at: www.r-project.org). Quantitative variables were expressed as means ± standard deviations. Categorical variables were expressed as frequencies or percentages. A Fisher exact test and a Pearson χ^2 test with Yates' continuity correction were used to measure the performance of guided review by frequent itemset mining in comparison with the guided review by a weighted random selection of segments. Because of the non-Gaussian distribution of the number of plaques per patient, a Mann-Whitney U test was performed to compare the average number of plaques in male and female patients. A $P < 0.05$ was considered statistically significant for all tests.

RESULTS

Coronary Artery Plaques

In 200 of 252 (79.4%) patients, at least one coronary plaque (range 1–22 plaques) was found. In total 1229 plaques (990 calcified, 80.6%; 227 mixed, 18.5%; 12 noncalcified, 1%) distributed, over 916 coronary segments and 507 vessels were manually labeled (Table 2). The average number of plaques for patients having at least one plaque was 6.1 (median 5).

Male patients had on average 6.9 plaques (5.6 calcified, 1.3 mixed, and 0.05 noncalcified plaques), being significantly ($P < 0.001$) more than the average in female patients (average 4.0, 3.3 calcified, 0.6 mixed, and 0.05 noncalcified).

Calcified and mixed plaques were most often found in segment 6 (132× calcified, 48× mixed), segment 1 (126× calcified, 34× mixed), and segment 7 (112× calcified, 25× mixed). Because of the few number of noncalcified plaques, no preferred location for those plaques could be concluded.

A total of 129 (10.5%) obstructive plaques (95 calcified, 31 mixed, 3 noncalcified) and 1100 (89.5%) nonobstructive plaques were detected in the 200 patients having plaques, as determined by CTCA. Obstructive plaques were most often located in segment 7 (23×), segment 6 (22×), and in segment 1 (18×) (see Table 2).

Spatial Plaque Distribution Patterns

Four special plaque distribution patterns could be identified in the 252 patients. Fifty-two of the 252 patients (20.6%) had no

TABLE 2. Plaque Distribution in the Study Population at 25 Possible Locations (Including Segments and Bifurcations) of the Coronary Artery Tree as Determined by CTCA

	All Plaques			Obstructive Plaques		
Segment/Bifurcation	**Calcified**	**Mixed**	**Noncalcified**	**Calcified**	**Mixed**	**Noncalcified**
1	126	34	3	11	6	1
1 × 2	2	1	0	1	0	0
2	73	11	2	5	2	1
2 × 3	0	0	0	0	0	0
3	80	20	0	5	1	0
3 × 4	0	0	0	0	0	0
4	45	9	0	0	0	0
5	70	21	1	5	1	0
5 × 11	0	0	0	0	0	0
6	132	48	2	16	6	0
6 × 9	3	1	0	1	0	0
7	112	25	1	18	5	0
7 × 10	1	1	0	0	1	0
8	78	11	2	1	2	1
9	27	5	1	3	1	0
10	20	4	0	3	2	0
11	78	15	0	10	3	0
11 × 12	1	0	0	0	0	0
12	25	4	0	3	0	0
13	54	9	0	10	1	0
13 × 14	0	0	0	0	0	0
13 × 15	0	0	0	0	0	0
14	19	0	0	1	0	0
15	16	1	0	1	0	0
16	28	7	0	1	0	0

plaques at all; 80 of the 252 patients (31.7%) had plaques only in the left coronary artery tree (ie, the LM, LAD, and CX); 117 of the 252 patients (46.4%) had plaques both in the left and the right coronary artery tree; and 3 of the 252 patients (1.2%) had plaques solely in the right coronary tree (Fig. 2).

Frequent Itemset Mining–Prediction Rules

Based on the labeled plaques, frequent itemset mining extracted a total of 70′796 prediction rules with a minimum confidence value of 80% and a minimum support of 15%. In general, there existed several rules showing evidence for a plaque at one and the same position. The differences between those rules were the amount of conditions but also the conditions themselves. Simple patterns were characterized by prediction rules with only one condition item (eg, segment 3 → segment 6 (24.6, 88.7)) whereas more specific patterns had multiple condition items (eg, segment 3 and CX → segment 6 (18.3, 91.3)). These specific patterns had higher confidence values. However, the support values decreased for more complex rules because their underlying plaque distribution patterns were less frequently observed in the patients.

The assignment of multiple items for each plaque allowed for a pattern analysis at (ie, vessel to vessel, segment to segment) and between different hierarchical levels (ie, segment to vessel and vice versa). In this study, we focused on plaque distribution patterns with prediction rules having one condition item. If multiple prediction rules fulfilled this criterion, the one with the highest confidence value was chosen.

All Plaques

Vessel to Vessel

General rules having a high support and confidence value were found indicating the existence of a plaque in the left anterior descending (LAD) given a plaque in any of the segments of the RCA. Furthermore, general rules supporting the existence of a plaque in the LAD, given a plaque in the CX or the left main artery (LM), were found (Table 3).

Segment to Segment

On this hierarchical level, a plaque in segment 3, 4, 5, 11, or 13 predicted a plaque in segment 6 with a high confidence (80.5% to 90.9%). Similarly, a plaque in segment 2 predicted a plaque in segment 1 with a high confidence (84.8%, see Table 3).

Segment to Vessel

Various rules predicting plaques in other vessels giving the existence of a plaque in certain segments were found: for example a plaque in segment 1, 2, 3, 5, 11, or 13 predicted a plaque in the LAD with high confidence (see Table 3).

Vessel to Segment

Rules predicting plaques in certain vessels based on existing plaques in other segments were found. For example, having a plaque in the CX, there was a confidence of 86.7% that also a plaque in

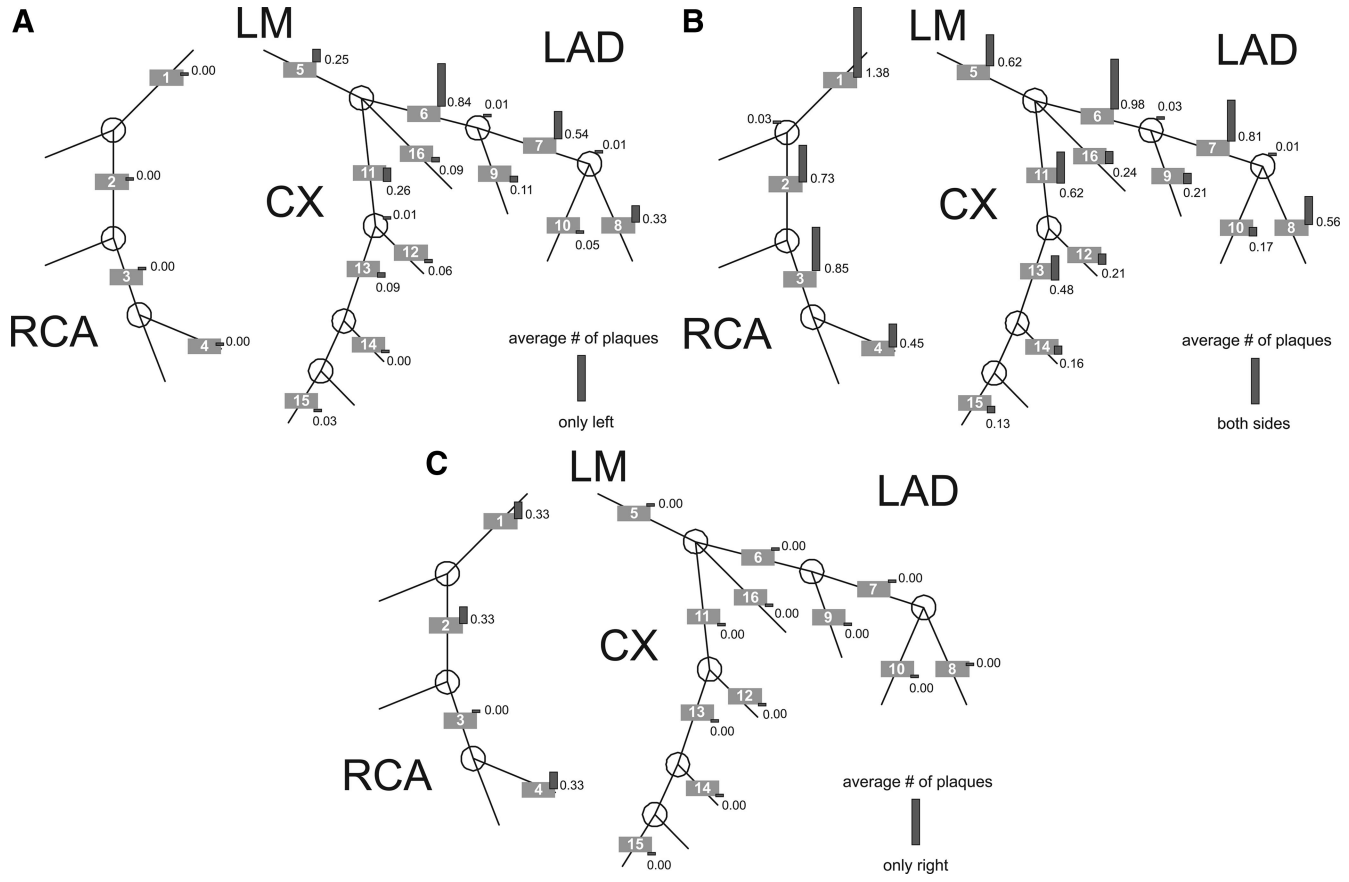

FIGURE 2. Schematic representation of the coronary artery tree (adapted from the AHA[25]) illustrating the spatial plaque distribution patterns in the 200 patients with coronary plaques. (A) in 31.7% of the patients, plaques were found only in the left coronary artery tree; (B) in 46.4% of the patients, plaques were found both in the left and the right coronary artery tree; (C) in 1.2% of the patients, plaques were located solely in the right coronary tree. The figures show the average number of plaques encountered in each segment of the coronary artery tree for each group separately.

segment 6 is present. A plaque in the LM predicted a plaque in segment 6 with a confidence of 80.5% (see Table 3).

Mixed and Noncalcified Plaques

For mixed plaques, no prediction rules were found using the minimum confidence value of 80% and one single condition item such that we lowered the confidence threshold to 65% and allowed for up to two condition items. Then several prediction rules were found to predict the existence of mixed plaques at the vessel level—ie, either within the right coronary tree (ie, RCA) or within the left coronary tree (ie, LM, LAD, or CX) (Table 4). No rules were found predicting mixed plaques in specific segments.

As only 12 noncalcified plaques were present in the patients of this study (representing 1% of all plaques), no relevant patterns or rules could be discerned with regard to this plaque type.

Guided Review

Based on the prediction rules extracted by frequent itemset mining, 193 segments in 133 patients were selected for the guided review. In these, an initially missed plaque was detected in 59 (30.6%) segments of 49 (36.8%) patients. From these 59 segments, 11 segments contained plaques extending over more than one segment such that those plaques were already labeled in the first reading with their most proximal segment position. Hence, in total 48 (24.9%) additionally detected plaques (32 calcified, 13 mixed, 3 noncalcified) in 41 (30.8%) patients were counted as true positives.

In comparison, the weighted random approach revealed only 22 (14 calcified, 5 mixed, 3 noncalcified) initially missed plaques in the 193 segments in 131 patients selected by this approach. Guided review by frequent itemset mining performed significantly better ($P < 0.001$) than the weighted random approach.

The distribution of additionally detected plaques over the various segments is illustrated in Fig. 3. The weighted random approach revealed 17 (77.3%) initially missed plaques in the left coronary tree and 5 (22.7%) in the right coronary tree. The results from frequent itemset mining were more balanced with 28 (58.4%) initially missed plaques in the left and 20 (41.6%) initially missed plaques in the right coronary tree, respectively.

DISCUSSION

It has been well documented through a number of epidemiological studies that human coronary atherosclerosis shows a nonuniform distribution in the coronary vasculature, not only among different coronary arteries, but also along different segments of the same vessel.[4,30] This article is, to the best of our knowledge-the first to describe spatial distribution patterns of coronary plaques by including the entire coronary artery tree into the analysis. The spatial

TABLE 3. Prediction Rules Including all Coronary Plaque Types Given an Existing Plaque as Condition and a Predicted Plaque at Certain Locations as Conclusion

Hierarchical Level	Existing Plaque	Predicted Plaque	Support Value (%)	Confidence Value (%)
Vessel → vessel	RCA	LAD	47.6	92.5
	LM	LAD	32.5	90.2
	CX	LAD	38.9	95.9
Segment → segment	Segment 2	Segment 1	26.2	84.8
	Segment 3	Segment 6	24.6	88.7
	Segment 4	Segment 6	15.1	86.8
	Segment 5	Segment 6	32.5	80.5
	Segment 11	Segment 6	28.6	87.5
	Segment 13	Segment 6	17.5	90.9
Segment → vessel	Segment 1	LAD	40.1	93.1
	Segment 2	LAD	26.2	90.9
	Segment 3	LAD	24.6	95.2
	Segment 4	LAD	15.1	92.1
	Segment 5	LAD	32.5	90.2
	Segment 11	LAD	28.6	95.8
	Segment 13	LAD	17.5	100.0
Vessel → segment	LM	Segment 6	32.5	80.5
	CX	Segment 6	38.9	86.7

plaque distribution patterns showed a predominance of plaques involving primarily the left coronary artery tree, whereas only 1% of the patients had plaques solely in the right coronary artery system. The observed patterns allowed for the extraction of prediction rules indicating the presence of plaques in certain positions when plaques in other locations of the coronary artery tree were present. In patients with chronic CAD, the prediction rules mainly involved plaques being entirely calcified and—to a lesser degree–plaques being of mixed composition. Use of these prediction rules significantly improved the manual detection of coronary plaques.

Spatial Plaque Distribution Patterns

So far, all studies analyzing the distribution of coronary plaques have evaluated the presence of plaques without considering a possible correlation among the localizations of different plaques within the coronary artery tree.[7,9,10,31,32] For example, the localization of occlusions,[7] stenoses,[32] ruptured plaques,[9,31] and thin cap fibroatheromas[31] have been studied. Moreover, the circumferential distribution pattern of plaques at bifurcations was assessed.[10] In this study, we sought to determine the spatial distribution patterns of coronary plaques whereas taking into account the entire coronary artery tree.

Three major spatial plaque distribution patterns could be identified in our patient population. One group (20.6% of the patients) had no plaques at all; another group (31.7% of the patients) had plaques in the left coronary artery tree (ie, the LM, LAD, and CX); whereas the largest group (46.4% of the patients) had plaques both in the left and the right coronary artery tree. Plaques solely located in the right coronary tree were observed in only 1.2% of the patients.

The frequent itemset mining algorithm extracted relationships between existing plaques and those that can be predicted with a certain confidence. Various general rules with a confidence above 90% were found predicting plaques in the LAD given plaques in the segments of the other coronary arteries. At the segment level, rules existed with a confidence between 80% to 90% that predicted plaques in the proximal LAD (segment 6) when plaques in different segments of the RCA, LM, or CX were present (see, Tables 3 and 4).

This altogether indicates that when a patient with chronic CAD shows plaques, these will primarily involve the LAD and only secondarily the other coronary arteries. The other way round, plaques in these patients involving any artery but not the LAD represents a very rare finding. In the latter case, a search for potentially overlooked plaques in the LAD should prompt the initial review.

A possible reason for the observed spatial plaque distribution patterns would be that the geometry of the left coronary artery tree influencing hemodynamic features such as wall shear stress would predispose the development of plaques more than does the geometry of the right coronary artery.[33] Another explanation could be a temporal evolution of plaque development, with plaques occurring first in the left coronary tree before developing later also in the right coronary artery system. The lower rate of plaques found in the RCA may also be attributable to the lower image quality in this vessel. As the RCA has a greater motion within a cardiac cycle than the left coronary tree, more blurring artifacts might be introduced that lower the image quality and therefore interferes with the detection of plaques.

In this study, prediction rules for mixed plaques were found only with a lower confidence (ranging between 60%–70%), and no prediction rules could be defined for noncalcified plaques. This most probably is related to the patients studied herein who are known to have a low prevalence for mixed and noncalcified plaques as compared with patients with unstable angina, acute coronary syndromes, or myocardial infarction.

Clinical Implications

The clinical implications for spatial plaque distribution patterns found in this study are manifold. As plaques have a prognostic value being independent of the presence or absence of luminal obstruction[21] they should be consistently detected in each CTCA study. Atherosclerotic disease is a process that involves various coronary segments.[4] The likelihood of coexisting additional segments with potentially symptomatic atherosclerosis has raised the question whether an interventional procedure directed to only one lesion should not tackle others as well. With regard to CTCA, it

TABLE 4. Prediction Rules for Mixed Plaques as Conclusion Given the Existence of Plaques (Calcified, Mixed, or Noncalcified) at Certain Locations as Conditions

Hierarchical Level	Existing Plaque	Predicted Mixed Plaque	Support Value	Confidence Value
Segments → branch	Segment 2 and 3	RCA	17.9	68.9
	Segment 6 and 8	Left coronary tree*	19.4	65.3
Segment and vessel → vessel	Segment 3 and LM	RCA	15.9	65.0
	RCA mixed and segment 6	Left coronary tree*	16.3	68.3

*Left coronary tree enclosing LM, LAD, CX, and segment 16, if present.

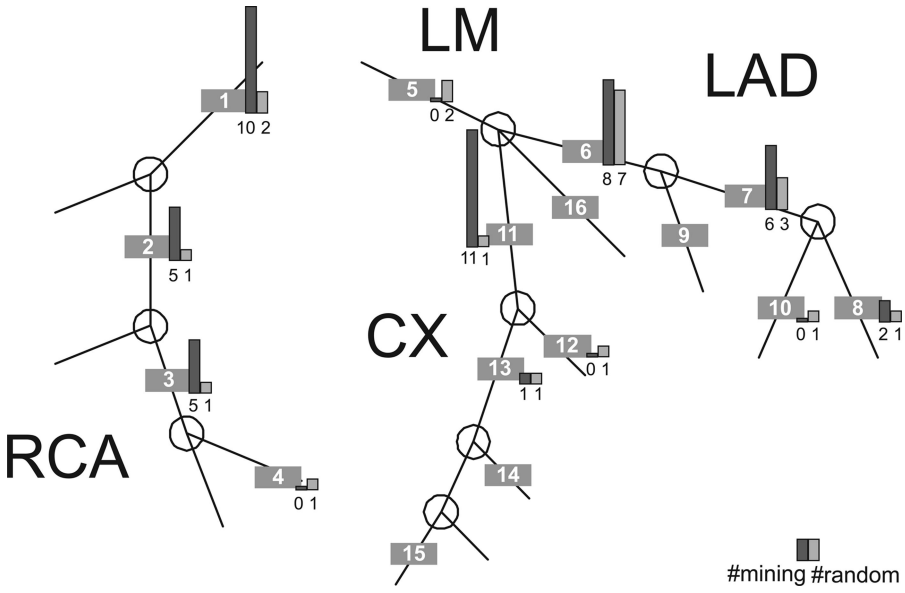

FIGURE 3. Schematic representation of the coronary artery tree indicating the number of plaques that were detected in the guided review by frequent itemset mining and in the weighted random approach. Guided review by frequent itemset mining performed significantly better ($P < 0.001$) than the random approach.

appears therefore mandatory to identify not only one, presumably obstructing plaque, but all plaques involving the entire coronary artery tree. This, however, as outlined above, can be difficult because of the lower performance of CT in comparison with the reference standard IVUS. Our study results giving rise to prediction rules help the interpreting radiologist through directing his review—once a plaque was found–to other coronary segments which are known to have a high probability to contain additional plaques.

As shown in the guided review, the prediction rules that encode observed spatial distribution patterns improve the plaque detection rate for manual labeling. Guided review can be used either as an online- or an offline-tool. As an online-tool, the current labeling would be automatically analyzed whereas the reader is still detecting plaques. Segments of potential plaque locations would be highlighted and continuously updated with the progress of manual labeling. As an offline-tool, the guided review would be manually triggered after the labeling and segments with potentially missed plaques would then be highlighted or listed in a table.

Finally, the prediction rules as determined in this study may be implemented in plaque detection software packages for improving their detection rate. Although automatic algorithms for plaque detection have been proposed,[34,35] their detection rates of 74% to 85% are still not optimal for routine clinical applications. In general, these algorithms use intensity-based features such that the detection of highly calcified plaques usually poses no problem. On the other hand, weakly calcified and noncalcified plaques are more challenging to detect. Thus, uncertainties may arise whether a slight intensity anomaly might be a plaque or not. When combined with an automatic segment labeling of the coronary artery tree, the detection algorithms may create additional evidence for the presence or absence of plaques in the uncertain segments by using the prediction rules in combination with the already detected plaques.

In this study, plaque distribution patterns from 252 patients have been learned and applied for the guided review. Considering the number of included patients, it is difficult to estimate an appropriate minimum number of patients for extending the study results to a broader patient population. At this point, variations in the spatial distribution patterns are not known such that a power analysis or other approaches are not feasible. As different populations with different clinical presentations show variable plaque type and distribution patterns, corresponding items for the populations and presentations should be created and assigned such that prediction rules from the respective subgroup can be chosen in the guided review process. The larger number of training data would also allow to research possible correlations between cardiovascular risk factors and specific spatial plaque distribution patterns.

Study Limitations

First, the plaques were labeled purely based on CTCA data with no correlation to IVUS. On the other hand, IVUS is not able to depict more distally located plaques, because of the diameter of the device. Therefore, an analysis of the spatial distribution of plaques including the entire coronary artery tree as performed in this study would not have been feasible with IVUS. Second, the initial labeling was performed by one reader such that observer variability was not determined. On the other hand, this has been previously documented in various studies.[22] Third, we did not measure the time for labeling the plaques in the first reading, nor did we measure the time for reviewing the data sets in the second reading. Fourth, we did not analyze possible relationships between spatial plaque distribution patterns and cardiovascular risk factors, because of the sample size of 252 patients being too low for this type of analysis. Finally, this study did not analyze the spatial plaque distribution patterns in patients with acute myocardial infarction or acute coronary syndromes.

CONCLUSION

This study describes spatial distribution patterns of coronary artery plaques based on CTCA data sets, which showed the plaques primarily involving the left coronary artery tree. Prediction rules were extracted to indicate the presence of plaques in certain positions when plaques in other locations of the coronary artery tree were present. Use of these prediction rules significantly improved the manual detection of coronary plaques.

ACKNOWLEDGMENT

The authors thank MeVis Research (Bremen, Germany) for supporting the study.

REFERENCES

1. Narula J, Garg P, Achenbach S, et al. Arithmetic of vulnerable plaques for noninvasive imaging. *Nat Clin Pract Cardiovasc Med*. 2008;5:S2–S10.

2. Ambrose JA, Winters SL, Stern A, et al. Angiographic morphology and the pathogenesis of unstable angina pectoris. *J Am Coll Cardiol*. 1985;5:609–616.
3. Shinohara M, Yamashita T, Tawa H, et al. Atherosclerotic plaque imaging using phase-contrast X-ray computed tomography. *Am J Physiol Heart Circ Physiol*. 2008;294:H1094–H1100.
4. Ehara S, Kobayashi Y, Yoshiyama M, et al. Spotty calcification typifies the culprit plaque in patients with acute myocardial infarction: an intravascular ultrasound study. *Circulation*. 2004;110:3424–3429.
5. Beckman JA, Ganz J, Creager MA, et al. Relationship of clinical presentation and calcification of culprit coronary artery stenoses. *Arterioscler Thromb Vasc Biol*. 2001;21:1618–1622.
6. Fujii K, Carlier SG, Mintz GS, et al. Intravascular ultrasound study of patterns of calcium in ruptured coronary plaques. *Am J Cardiol*. 2005;96:352–357.
7. Wang JC, Normand SLT, Mauri L, et al. Coronary artery spatial distribution of acute myocardial infarction occlusions. *Circulation*. 2004;110:278–284.
8. Hong MK, Mintz GS, Lee CW, et al. Plaque ruptures in stable angina pectoris compared with acute coronary syndrome. *Int J Cardiol*. 2007;114:78–82.
9. Pregowski J, Tyczynski P, Mintz GS, et al. Intravascular ultrasound assessment of the spatial distribution of ruptured coronary plaques in the left anterior descending coronary artery. *Am Heart J*. 2006;151:898–901.
10. Shimada Y, Courtney BK, Nakamura M, et al. Intravascular ultrasonic analysis of atherosclerotic vessel remodeling and plaque distribution of stenotic left anterior descending coronary arterial bifurcation lesions upstream and downstream of the side branch. *Am J Cardiol*. 2006;98:193–196.
11. Leber AW, Becker A, Knez A, et al. Accuracy of 64-slice computed tomography to classify and quantify plaque volumes in the proximal coronary system: a comparative study using intravascular ultrasound. *J Am Coll Cardiol*. 2006;47:672–677.
12. Hiro T, Leung CY, De Guzman S, et al. Are soft echoes really soft? Intravascular ultrasound assessment of mechanical properties in human atherosclerotic tissue. *Am Heart J*. 1997;133:1–7.
13. Palmer ND, Northridge D, Lessells A, et al. In vitro analysis of coronary atheromatous lesions by intravascular ultrasound. Reproducibility and histological correlation of lesion morphology. *Eur Heart J*. 1999;20:1701–1706.
14. Johnson TRC, Nikolaou K, Busch S, et al. Diagnostic accuracy of dual-source computed tomography in the diagnosis of coronary artery disease. *Invest Radiol*. 2007;42:684–691.
15. Stein PD, Beemuth A, Kayali F, et al. Multidetector computed tomography for the diagnosis of coronary artery disease: a systematic review. *Am J Med*. 2006;119:203.
16. Rist C, Johnson TR, Müller-Starck J, et al. Noninvasive coronary angiography using dual-source computed tomography in patients with atrial fibrillation. *Invest Radiol*. 2009;44:159–167.
17. Hoffmann U, Moselewski F, Nieman K, et al. Noninvasive assessment of plaque morphology and composition in culprit and stable lesions in acute coronary syndrome and stable lesions in stable angina by multidetector computed tomography. *J Am Coll Cardiol*. 2006;47:1655–1662.
18. Achenbach S, Moselewski F, Ropers D, et al. Detection of calcified and noncalcified coronary atherosclerotic plaque by contrast-enhanced, submillimeter multidetector spiral computed tomography: a segment-based comparison with intravascular ultrasound. *Circulation*. 2004;109:14–17.
19. Hausleiter J, Meyer T, Hadamitzky M, et al. Prevalence of noncalcified coronary plaques by 64-slice computed tomography in patients with an intermediate risk for significant coronary artery disease. *J Am Coll Cardiol*. 2006;48:312–318.
20. Iriart X, Brunot S, Coste P, et al. Early characterization of atherosclerotic coronary plaques with multidetector computed tomography in patients with acute coronary syndrome. *Eur Radiol*. 2007;17:2581–2588.
21. Pundziute G, Schuijf JD, Jukema JW, et al. Prognostic value of multislice computed tomography coronary angiography in patients with known or suspected coronary artery disease. *J Am Coll Cardiol*. 2006;49:62–70.
22. Hoffmann H, Frieler K, Hamm B, et al. Intra- and interobserver variability in detection and assessment of calcified and noncalcified coronary artery plaques using 64-slice computed tomography. *Int J Cardiovasc Imaging*. 2008;24:735–742.
23. Leschka S, Scheffel H, Desbiolles L, et al. Image quality and reconstruction intervals of dual-source CT coronary angiography: recommendations for ECG-pulsing windowing. *Invest Radiol*. 2007;42:543–549.
24. Leschka S, Alkadhi H, Stolzmann P, et al. Mono- versus bisegment reconstruction algorithms for dual-source computed tomography coronary angiography. *Invest Radiol*. 2008;43:703–711.
25. Austen WG, Edwards JE, Frye RL. A reporting system on patients evaluated for coronary artery disease. Report of the Ad Hoc Committee for Grading of Coronary Artery Disease, Council on Cardiovascular Surgery, American Heart Association. *Circulation.* 1975:5–40.
26. Asakura T, Karino T. Flow patterns and spatial distribution of atherosclerotic lesions in human coronary arteries. *Circ Res*. 1990;66:1045–1066.
27. Agrawal R, Imieliński T, Swami A. Mining association rules between sets of items in large databases. In: *SIGMOD '93: Proceedings of the 1993 ACM SIGMOD International Conference on Management of Data.* Washington, DC: 1993;207–216.
28. Saur SC, Alkadhi H, Desbiolles L, et al. Guided review by frequent itemset mining: additional evidence for plaque detection. *Int J CARS*. 2009;4:263–271.
29. Borgelt C, Kruse R. Induction of association rules: a priori implementation. In: *15th Conference on Computational Statistics* 2002. Berlin, Germany: 2002; 395–400.
30. Zhu H, Ding Z, Piana RN, Gehrig TR, Friedman MH. Cataloguing the geometry of the human coronary arteries: a potential tool for predicting risk of coronary artery disease. *Int J Cardiol.* 2008. In press.
31. Cheruvu PK, Finn AV, Gardner C, et al. Frequency and distribution of thin-cap fibroatheroma and ruptured plaques in human coronary arteries: a Pathologic Study. *J Am Coll Cardiol*. 2007;50:940–949.
32. Maehara A, Mintz GS, Castagna MT, et al. Intravascular ultrasound assessment of the stenoses location and morphology in the left main coronary artery in relation to anatomic left main length. *Am J Cardiol*. 2001;88:1–4.
33. Friedman MH, Deters OJ, Mark FF, et al. Arterial geometry affects hemodynamics. A potential risk factor for atherosclerosis. *Atherosclerosis*. 1983;46:225–231.
34. Isgum I, Rutten A, Prokop M, et al. Detection of coronary calcifications from computed tomography scans for automated risk assessment of coronary artery disease. *Med Phys*. 2007;34:1450–1461.
35. Saur S, Alkadhi H, Desbiolles L, et al. Automatic detection of calcified coronary plaques in computed tomography data sets. In: *Medical Image Computing and Computer-Assisted Intervention - MICCAI* 2008. Berlin, Germany: Springer; 2008:170–177.

